Journal of Marine Science and Technology, Vol. 24, No. 6, pp. 1146-1154 (2016)
DOI: 10.6119/JMST-016-1026-3

A COMPUTATIONAL STUDY ON SENSOR LOCALIZATION FOR UNDERWATER ACOUSTIC SENSOR NETWORK IN THE EAST SEA ENVIRONMENTAL MODEL

Jinyoung Choi, Kiseon Kim, and Sung Chan Jun

Key words: underwater acoustic sensor networks, sensor localization, deep water, sound speed profile, ray tracing.

ABSTRACT

An underwater acoustic sensor network (UASN) is a promising method for surveillance or monitoring underwater environments. This network may be most applicable as a disaster alarm system against tsunamis and red tides. Sensor measurement data and sensor location information from these networks are important elements for the UASN system. However, global positioning system (GPS) information is not yet available because the electromagnetic signal has high attenuation under the water. Thus, new methods for sensor localization are of great importance to UASN systems.

In this paper, an event-driven localization scheme using the constant arrival time surface (ELSUCATS) is proposed to achieve a more accurate sensor localization, which is an essential element in a warning system used to detect seasonal events, for example, a red tide or a tsunami. By considering the East Sea of South Korea where the red tides occur frequently in the summer, an underwater configuration (1000 m × 1000 m × 600 m) and sound speed profiles (SSPs) that depend on depth were modelled for testing.

Our proposed scheme shows that even for a noisy and large depth variation of SSP, the localization success ratio is still over 94% on average, and the mean error ratio is less than 0.0011. This demonstrates that our scheme has outperformed the conventional reverse localization scheme (RLS) in accuracy and is strongly robust to measurement errors and sound speed variations.

I. INTRODUCTION

Paper submitted 05/30/15; revised 09/01/16; accepted 26/10/16. Author for correspondence: Sung Chan Jun (e-mail: scjun@gist.ac.kr).
School of Electrical Engineering and Computer Science, Gwangju Institute of Science and Technology, Gwangju, South Korea.

1. Localization of an Underwater Acoustic Sensor Network

The underwater acoustic sensor network (UASN) is an appealing method for the real-time surveillance and monitoring of an underwater environment. A UASN may be applicable as an early warning system for disasters such as tsunamis, red tides, and similar disasters. Various types of sensor information are provided by a UASN, such as temperature, saltiness, and pressure. However, in an underwater environment, the global positioning system (GPS) information from the sensors is not available because the electromagnetic signal has a high attenuation property due to the conductivity of the water (Sozer et al., 2000). Therefore, for communication via a UASN, the acoustic signal is commonly used because it has a low attenuation rate in the water. An acoustic signal is typically composed of both time information and sensor measurements or event detection information. However, these sensor measurements may be useless until the exact positions of the sensors are determined (Teymorian et al., 2009). Therefore, sensor localization is an important technique for maintaining the usability of a UASN.

Sensor localization schemes are classified into either range-based schemes or range-free schemes. The former need additional hardware, but they yield a more accurate estimation of sensor positioning. The latter require relatively lower network costs than range-based schemes, but they yield relatively lower spatial resolution in sensor position estimation. In particular, principal range-based localization schemes such as received signal strength (RSS), time of arrival (ToA), and angle of arrival (AoA), are widely used.

The ToA scheme is based on the relationship between the traveling time of the acoustic signal and the sound speed profile in the underwater environment (Dargie and Poellabauer, 2010). Using the sound speed profile information, the acoustic ray path can be traced with the information of the sound source location and the initial sound ray emission angle. While tracing the ray, acoustic wave bending (ray bending) appears due to the sound speed profile variation in the underwater environment. This underwater bending phenomenon is negligibly small for a short distance, but it is notable over a longer distance, particularly in

a deep and broad underwater environment. Therefore, ray bending should be concerned with getting a more accurate distance between the sensors in a large-scale UASN.

However, without considering the bending phenomenon, the constant sound speed has been assumed in the most recent studies (Zhou et al., 2007; Isik and Akan, 2009; Moradi et al., 2012). These approaches may yield a non-negligible amount of sensor distance error due to the ray bending phenomenon. Thus, this sizable distance error may be propagated and result in substantial degradation of the localization performance. According to this reasoning, a realistic variation of the sound speed profile should be considered in a UASN to make the sensor localization more precise.

1. Related Work

Zhou et al. (2007) studied the localization problem in a large-scale underwater sensor network composed of 500 sensor nodes. These nodes were assumed to be randomly located in a 100 m × 100 m × 100 m cubical region. The researchers considered two types of sensor nodes: anchor nodes that are found or informed location initially on the surface of the sea and ordinary underwater sensor nodes. Anchor nodes emit localization messages periodically, and ordinary sensor nodes emit event-detecting information. Using an iterative algorithm, the location of ordinary sensor nodes were sought with the ToA scheme. However, a constant sound speed (average sound speed value over the whole region) was considered and thus the realistic variations of the sound speeds over depths could not be reflected.

Moradi et al. (2012) proposed an event-driven localization scheme called the reverse localization scheme (RLS) that was triggered by sensor nodes for launching the localization process. With a broad and deep environment (1000 m × 1000 m × 600 m), they performed their localization evaluation by varying the number of underwater sensor nodes and surface anchor nodes. However, they set the sound speed value as a constant value (average of estimated sound speed), even though the surface anchor nodes and underwater sensor nodes communicated directly. Thus, RLS may be prone to yielding a localization error caused by ray bending during long-range sound signal propagation.

Ameer and Jacob (2010) presented a scheme that takes into account a constant arrival time for the surface, which is collection of points whose arrival times of the acoustic signal from the source are identical. Using this given time of arrival (ToA) information, surfaces for known nodes in the center are generated, and seeking the intersection (or the point that has a minimum sum of distances from the three surfaces) of these surfaces is done to yield the sensor nodes' localization. This scheme yielded a reasonably accurate node localization performance. However, the test bed for the simulation was a 150 m × 150 m × 90 m water body, which is too small scale.

Isik and Akan (2009) proposed three-dimensional underwater localization (3DUL) by using an iteration algorithm with a sensor projection. They exploited only three surface anchor nodes for localization. From that initial state, 3DUL spread the global position knowledge across the network by an iterative scheme. They assumed that the sensor nodes were equipped with conductivity, temperature, and depth (CTD) sensors. During the localization sequence, they used the depth information for the sensor node projection. For the sound speed profile measurement, an empirical equation was introduced (Mackenzie, 1981). Even though this approach helped to get a more accurate sound speed profile, the realistic sound speed variation could not be reflected because they used the average sound speed value.

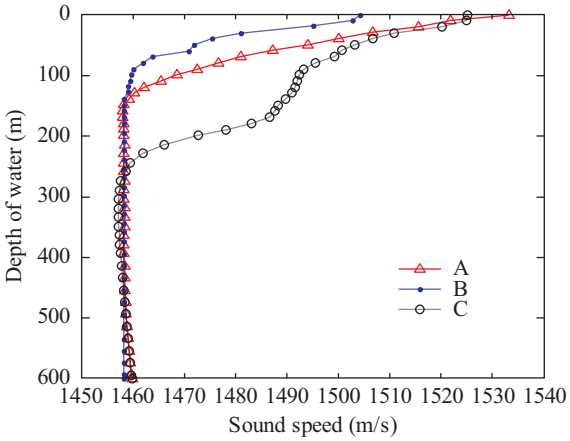

Fig. 1. Three exemplary sound speed profiles (SSPs) in the East Sea environment. These are typical patterns observed in summer.

In this study, we attempted to simulate the UASN localization problem in the East Sea environment model (depth of over 500 m). During the summer, the red tide occurs frequently in the East Sea of South Korea. A warning system for the red tide or an abnormally warm current detector system may be greatly beneficial to the fishing operations in that area.

We observed that the sound speed profile of the East Sea varies drastically by depth, as illustrated in Fig. 1. Thus, in this environment, acoustic ray bending which occur during underwater communication between sensors may be substantially significant. Therefore, underwater sensor localization in the East Sea environment should consider the sound speed profile variation. In line with this reasoning, we propose an event-driven localization scheme using a constant arrival time surface (ELSUCATS), which is a hybrid approach between Moradi's scheme and Ameer's algorithm. In this work, the feasibility of the warning system using a UASN with ELSUCATS in the East Sea was mainly investigated. We note that the BELLHOP ray-tracing program developed by Porter and Bucker (1987) was modified for our purposes.

II. SYSTEM STRUCTURE

1. Architecture of Acoustic Sensor Network

In this study, our acoustic sensor network is composed of un derwater sensor nodes, surface anchor nodes, and an onshore sink (Fig. 2). The nodes monitor predefined events such as ab-

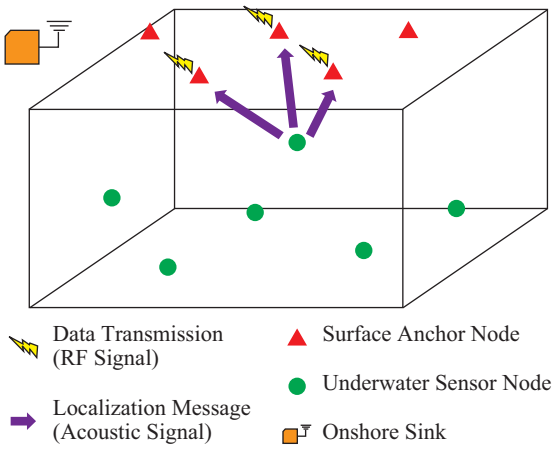

Fig. 2. Underwater acoustic sensor network architecture for ELSUCATS.

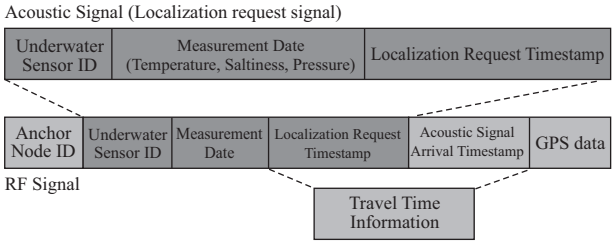

Fig. 3. Packet Transmission Structure for ELSUCATS.

normally high underwater temperature. Every node was assumed to be equipped with temperature, saltiness, and pressure sensors. Depth information for each sensor node is obtainable by an equipped pressure sensor. The nodes use an acoustic signal transmitter for communicating and broadcasting localization requests in omnidirectional way when a predefined event is detected. A localization request signal is composed of measurement data, such as temperature, saltiness, and pressure, and timestamp information as shown in Fig. 3.

We assume that the surface anchor nodes float on the surface of the water are equipped with "GPS receivers" determining global sensor position, "long-range radio frequency (RF) signal transceivers" for communicating with an onshore sink and "acoustic signal receivers" detecting the localization request signal from the underwater sensor nodes. The RF signal contains the GPS information of the anchor node, the arrival time stamp of acoustic signals, and packets from the acoustic signals (measurement data and localization request timestamp).

Lastly, an onshore sink receives the RF signal from the anchor nodes to collect the global position information of the anchor nodes and the traveling time of the localization request signals. An onshore sink was assumed to be furnished with a database of event-detecting sensor information and embedded with an algorithm for sensor localization, which may be performed on a real-time basis.

2. Process of Event Detection and Response

Underwater sensor nodes monitor their environment. When a sensor node detects a predefined event, it immediately emits a localization request signal to the surface anchor nodes through the acoustic signal. These anchor nodes wait for any localization requests from the underwater nodes. After sensing this signal, the anchor nodes immediately transmit an RF signal that consists of the anchor node's global position and timestamp data for measuring the traveling time of the localization request signal. The system clock is assumed to be synchronized for all sensor nodes. Therefore, traveling time can be measured by the difference between a localization request timestamp (recorded by the detector sensor node) and an arrival timestamp of a localization request signal (recorded by the anchor node). An onshore sink processes the sensor localization with this received information. Using the sound speed profile data, the wavefront from the acoustic signal source can be measured by ray-tracing. Therefore, if the collected information about the location of the anchor node and traveling time from at least three anchor nodes is provided, then the wavefront surfaces from each anchor node can be constructed as shown in Fig. 4. The intersections of wavefront surfaces and a sensor depth plane, indicated by circles with a dashed line in Fig. 4, are estimated for localization, then trilateration is conducted with these circles. When event-detector sensor localization is done successfully, the system may issue an alarm as scheduled for disaster prevention or a surveillance objective.

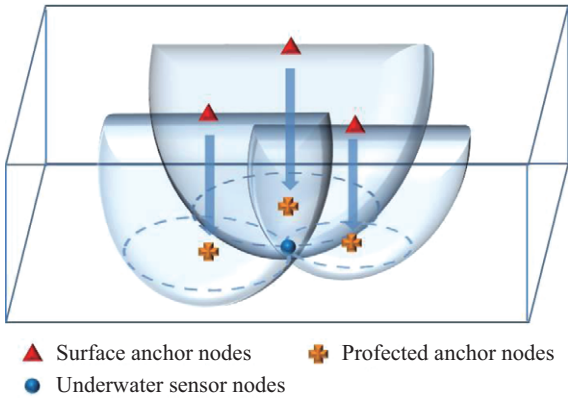

Fig. 4. An example of three constant arrival time surfaces and projection of anchor nodes into the sensor depth plane.

In this work, we note that the system response time was defined as the elapsed time from an event detection to the final sensor localization success.

III. METHOD

1. Localization Algorithm

An underwater acoustic sensor broadcasts the localization request when an event is detected, which is a typical initiation of the event-driven localization scheme (Moradi et al., 2012). Then the surface anchor nodes listen to the localization request signal. For each anchor node, the arrival time of the localization request signal is recorded as reporting. Three or more anchor nodes reporting the shortest arrival times and showing a non-

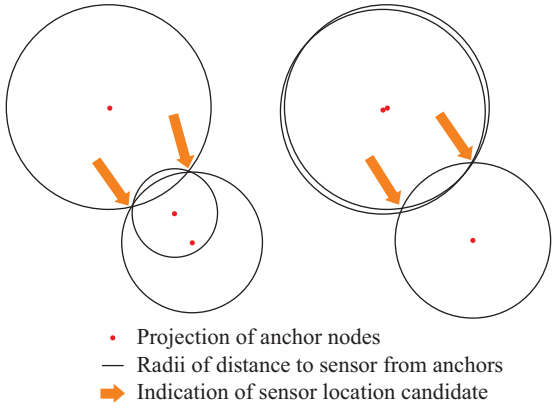

Fig. 5. Localization examples with collinear anchor arrangement; the intersection of three circles is not unique.

collinear arrangement are selected for localization. We note that the selection of anchor nodes forming almost a collinear arrangement may yield an ambiguous sensor localization result (Fig. 5). Therefore, three anchor nodes yielding the far-away collinear arrangement may be a reasonable set among the surface anchor nodes for the trilateration. From these three anchor nodes, acoustic ray propagation can be modeled. A collection of all points having the same signal traveling time forms a constant arrival time surface (Ameer and Jacob, 2010). Fig. 4 depicts an example of constant arrival time surfaces and illustrates three circles, which are the intersections of the constant arrival time surfaces and the depth planes of a detector sensor.

Using three radii of circles, the following three equations are obtained:

$$\begin{aligned}(A_{1X}-S_X)^2 + (A_{1Y}-S_Y)^2 &= R_1^2\\ (A_{2X}-S_X)^2 + (A_{2Y}-S_Y)^2 &= R_2^2\\ (A_{3X}-S_X)^2 + (A_{3Y}-S_Y)^2 &= R_3^2\end{aligned} \tag{1}$$

where (A_{iX}, A_{iY}) is i-th surface anchor location, (S_X, S_Y) is an underwater sensor location, and R_i is the radius of each circle. Subtracting the third equation from the first and the second equations yield the following two equations:

$$\begin{aligned}&A_{1X}^2 - A_{3X}^2 + A_{1Y}^2 - A_{3Y}^2 - 2S_X(A_{1X}-A_{3X})\\ &\quad - 2S_Y(A_{1Y}-A_{3Y})^2 = R_1^2 - R_3^2\\ &A_{2X}^2 - A_{3X}^2 + A_{2Y}^2 - A_{3Y}^2 - 2S_X(A_{2X}-A_{3X})\\ &\quad - 2S_Y(A_{2Y}-A_{3Y})^2 = R_2^2 - R_3^2\end{aligned} \tag{2}$$

Eq. (2) can be re-expressed as the following linear system

$$\mathbf{A}\vec{x} = \vec{b} \tag{3}$$

where

$$\vec{x} = \begin{bmatrix} S_X \\ S_Y \end{bmatrix}, \mathbf{A} = \begin{bmatrix} 2(A_{1X}-A_{3X}) & 2(A_{1Y}-A_{3Y}) \\ 2(A_{2X}-A_{3X}) & 2(A_{2Y}-A_{3Y}) \end{bmatrix}$$

$$\vec{b} = \begin{bmatrix} A_{1X}^2 - A_{3X}^2 + A_{1Y}^2 - A_{3Y}^2 - R_1^2 + R_3^2 \\ A_{2X}^2 - A_{3X}^2 + A_{2Y}^2 - A_{3Y}^2 - R_2^2 + R_3^2 \end{bmatrix}$$

Then this system is solved in a least square sense to get the estimation of a sensor node location by trilateration (Liu et al., 2010) as follows:

$$\vec{x} = (\mathbf{A}^T\mathbf{A})^{-1}\mathbf{A}^T\vec{b} \tag{4}$$

This result may be used as an initial point for the searching algorithm in order to finally find the local optimal point, which indicates the minimum distance to three constant arrival time surfaces.

Our scheme may give a more precise sensor localization because the sound speed profile is considered using constant arrival time surface, even though scheme proceeds with the event-driven localization concept in quite a long communication range.

2. Local Search

From the least square solution (Eq. (4)), our local grid search was initiated as follows. First, a 41 × 41 grid with a 1-m resolution centered at initial point (the least square solution) was generated. For every grid point, a distance summation from the three constant arrival time surfaces was estimated; this distance summation is defined as a cost function for optimization process. After the completion of the distance summation for all grid points, we moved to the point yielding the smallest distance summation value from three surfaces. Again, at this point, we generated a 41 × 41 grid within a 2 m × 2 m area (50 mm resolution). Then the same procedure was repeated to find the point yielding the smallest distance. This search algorithm was stopped after the third grid search, where the spatial resolution of gird is 2.5 mm, which is small enough.

3. Performance Evaluation

For the quantitative analysis, a confidence value is introduced as follows (Erol-Kantarci et al., 2011):

$$\sigma = \begin{cases} 1, & \text{for anchor nodes} \\ 1 - \dfrac{\sum_{i=1}^{n}\left|(S_X-A_{iX})^2 + (S_Y-A_{iY})^2 + S_Z^2 - d_i^2\right|}{\sum_{i=1}^{n}(S_X-A_{iX})^2 + (S_Y-A_{iY})^2 + S_Z^2}, & \text{otherwise} \end{cases} \tag{5}$$

where (S_X, S_Y, S_Z) is an underwater sensor node location, (A_{iX}, A_{iY}) is *i-th* surface anchor node location, and d_i is an exact distance between the sensor node and the *i-th* anchor node. We note that anchor nodes are assumed to be on the water's surface; thus the z-component is considered as zero, that is, $A_{iZ} = 0$.

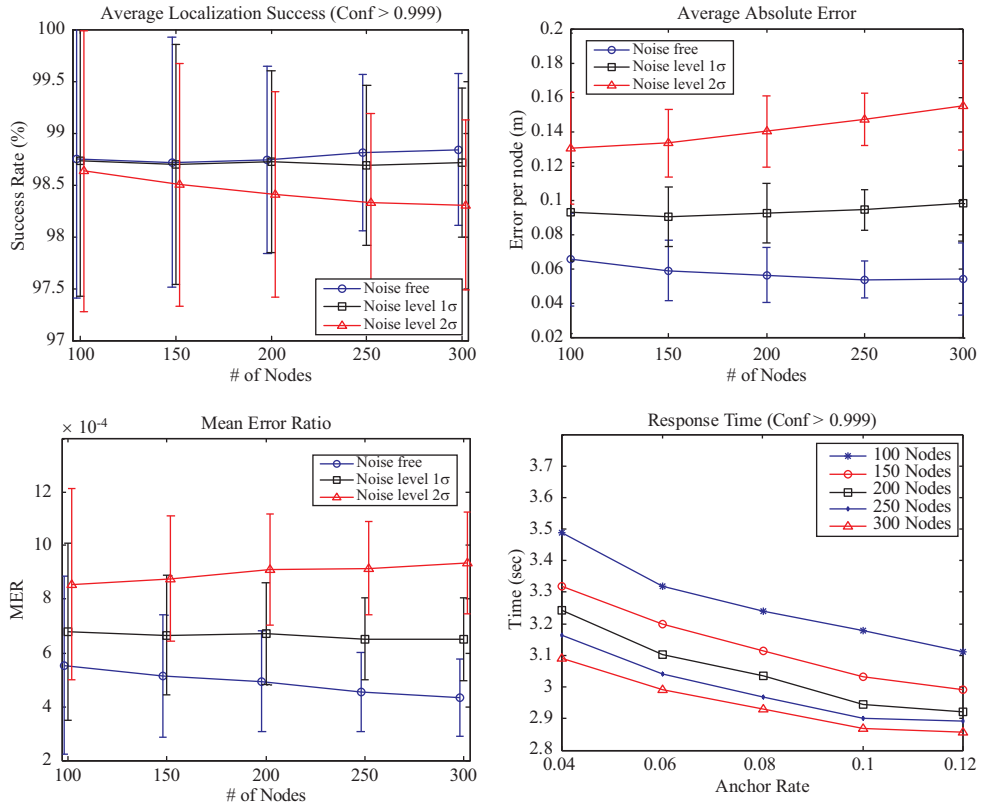

Fig. 6. Simulation results of the UASN localization with a timestamp error; localization success rate (upper left), absolute error (upper right), mean error ratio (lower left), and system response time (lower right).

A threshold of confidence value for declaring the success of a localization process was set to 0.999 in this study. Thus, cases yielding a confidence value of less than 0.999 were considered as localization failure.

To evaluate the localization performance, Moradi's average localization success (Avg_{LS}) and mean error ratio (MER) were introduced as follows:

$$Avg_{LS} = \frac{\sum_{i=1}^{n} N_{L,i}}{n} \tag{6}$$

$$MER = \frac{\sum_{i=1}^{n} ((X_i - \hat{X}_i)^2 + (Y_i - \hat{Y}_i)^2 + (Z_i - \hat{Z}_i)^2)/Z_i}{n} \tag{7}$$

Here $N_{L,i}$ is the number of localization successes for trial i and n is the number of trials. (X_i, Y_i, Z_i) and $(\hat{X}_i, \hat{Y}_i, \hat{Z}_i)$ are a true sensor node location and an estimated sensor node location, respectively (Moradi et al., 2012).

IV. SIMULATION

1. Simulation Setup

Table 1. Simulation Parameters for Method Evaluation.

Parameter	Value
Localization domain	1000 m × 1000 m × 600 m
Signal frequency	25 kHz
Number of underwater sensor nodes	{100, 150, 200, 250, 300}
Surface anchor ratio at sensor nodes	{4%, 6%, 8%, 10%, 12%}
Noise level in arrival time	{0, 1σ, 2σ, 5σ, 10σ}, σ = 1.5 × 10^{-6} sec
Depth sensor error	{0, 1σ}, σ = 0.1 m
Simulation run	50

To investigate the feasibility of our proposed event-driven localization scheme using constant arrival time surfaces (ELSUCATS), a UASN environment was modelled as realistically as possible. The parameters used in this model are listed in Table 1. Underwater sensor nodes were distributed randomly in 1000 m × 1000 m × 600 m regions, and anchor nodes were distributed randomly on the upper surface (representing the water surface) of the model.

Signal frequency was considered as 25 kHz, which is applicable for roughly a 1.0-km range communication (Moradi et al., 2012).

The number of underwater sensor nodes varied from 100 to 300, and the number of surface anchor nodes varied from 4%

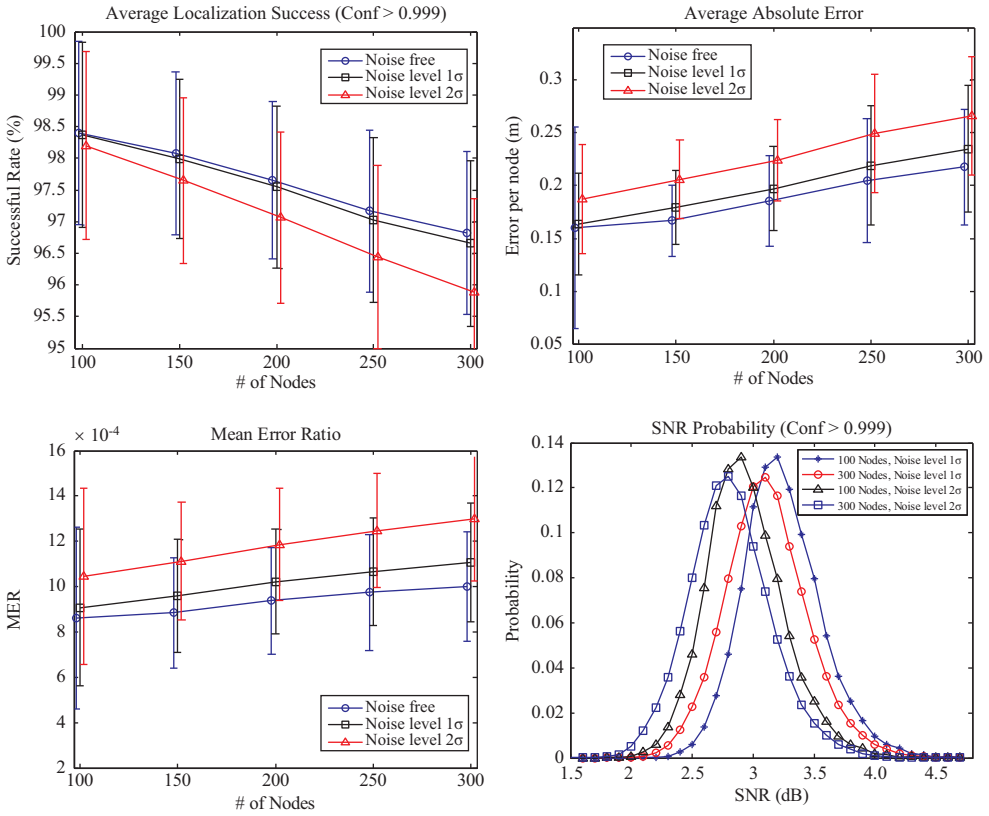

Fig. 7. Performance evaluation with depth error; localization success rate (upper left), absolute error (upper right), mean error ratio (lower left) and signal to noise probability distribution of depth error-free case (lower right).

to 12% of the given number of sensor nodes. Noise-free and noisy cases were considered by adding zero mean Gaussian noise to the original arrival time. The standard deviation of arrival time noise was introduced at 1.5 micro-seconds, as used in the previous work (Moradi et al., 2012).

We also considered the probable depth error from pressure sensors for underwater sensors as the zero mean Gaussian noise with standard deviation of 0.1 m (Moradi et al., 2012). Trials were tested for 50 noisy and 50 noise-free cases. For each trial, underwater sensor nodes and anchor nodes were re-distributed randomly.

The East Sea's sound speed profile data were obtained from the ocean data portal of Korea Institute of Ocean Science and Technology (KIOST), as shown in Fig. 1. It is noted that this sound speed profile was estimated by the formulation depending on temperature, saltiness and pressure variables (King et al., 2008). The sound speed of the East Sea varied drastically by depth. We noted that the average computation time for a localization simulation was 7.48 seconds using MATLAB on our computing resource (Quad core Intel i7 64 bit, 3.5 GHz workstation with 8 GB RAM)

2. Method Evaluation

With 50 trials of UASN localization using ELSUCATS, the localization performance was compared over three different noise levels (0σ, 1σ, and 2σ). We note that simulation results for a representative SSP data (B in Fig. 1) were presented only in this section. Fig. 6 shows the performance evaluation results of the UASN localization simulation with timestamp noise (localization success rate, mean error ratio, absolute error, and system response time).

ELSUCATS showed an overall steady performance (over a 98.3% success rate on average), even though localization performance for highly noisy case (+2σ) was slightly degraded as the number of nodes increased. That is, our scheme showed robustness to the small noisy case (+σ). The average absolute localization error of our scheme was achieved roughly 6 cm for noise free cases. In addition, the mean error ratio in our scheme was achieved as lower than 0.0006 with the noise-free case and 0.0009 with noisy case (+2σ).

In Fig. 6, the system's response time yielded a gradual decrease as the number of sensor nodes (both underwater sensors and surface anchors) increased. Particularly, observing 250 or more sensor nodes and 8% or more anchor ratios, the decrease in response time looks marginal. Thus, under our experimental setting, 250 sensor nodes and 20 anchor nodes (8% of anchor ratio) would be good enough to test the localization performance in terms of response time.

Finally, considering the depth sensing error, the localization performance was investigated. Compared with the depth error-free simulation results, the expected overall performance decreased (Fig. 7); averaged localization success rate decreased

Table 2. Simulation Parameters for Benchmark Study.

Parameter	Value
Localization domain	1000 m × 1000 m × 600 m (Moradi et al.)
	150 m × 150 m × 90 m (Ameer and Jacob)
Signal frequency	25 kHz
Number of underwater sensor nodes	(100, 150, 200, 250, 300)
Surface anchor ratio at sensor nodes	(8%)
Noise level in arrival time	(1σ), $\sigma = 1.5 \times 10^{-6}$ sec
Depth sensor error	(1σ), σ = 0.1 m
Simulation run	25

Table 3. Simulation Results for Benchmark Study.

Method	ELSUCATS			Common ToA		
Sound Speed Profile	A	B	C	A	B	C
Average Success Rate (%) (confidence value > 0.999)	97.2	98.9	94.2	26.2	54.8	10.1
Average Absolute Error (m)	0.09	0.09	0.18	3.06	1.65	6.71
Average Mean Error Ratio	0.0005	0.0006	0.0011	0.027	0.036	0.086

from 98.3% to 95.8%, averaged localization error increased from 15 cm to 26 cm, and mean error ratio rose from about 0.0009 to 0.0013. Therefore, it may be inferred that the depth sensing error seems to be more sensitive to localization accuracy than other factors.

3. Comparative Study with Existing Methods

For a performance comparison with existing methods, we investigated the comparative studies under the same computational configurations. The common ToA method (reverse localization scheme, RLS) reported by Moradi et al. (2012) was compared with our proposed ELSUCATS.

Parameters used in this comparison are listed in Table 2. The conventional timestamp noise level and depth sensor error level were set to 1.5 micro-seconds and 0.1 micro-seconds, respectively. Underwater sensor nodes were distributed randomly in 1000 m × 1000 m × 600 m regions and anchor nodes were distributed randomly on the upper surface of the model. The number of underwater sensor nodes varied from 100 to 300, and the number of surface anchor nodes was set to 8% of the given number of sensor nodes. Twenty-five trials were conducted and underwater sensor nodes and anchor nodes were re-distributed randomly for each trial. In addition, to see the influence of different sound speed profiles on the sensor localization performance, three SSPs (Fig. 1) were tested for comparison.

Our proposed ELSUCATS consistently far outperformed the common ToA method for three typical SSPs. Average success rates in ELSUCATS yielded over 94%, while those in the common ToA method were substantially lower and varied from about 10% to 26%. For average absolute error, ELSUCATS yielded 0.18 m or lower, while the common method yielded quite large variation between 1.65 m and 6.71 m. Overall, ELSUCATS was 60 times better in average MER than the common ToA method. Detailed comparative results over three SSPs are tabulated in Table 3 and illustrated in Fig. 8.

It was observed that the larger variation of the sound speed profile by depth yielded the greater performance degradation of the common ToA method, compared to our proposed ELSUCATS. This is supportive that a constant sound speed is not reasonable in a drastic sound speed variation environment. In the meantime, even though for largest variation of SSP by depth (C in Fig. 8), both methods showed the worst performance, ELSUCATS gave more robustness to the sound speed variation than the common ToA method. Interestingly, we observed that the number of sensor nodes had some influence on localization performance in the common ToA method, while ELSUCATS showed steady localization performance over varying the number of sensor nodes (Fig. 8, upper right).

Ameer and Jacob (2010) tested their method in a 150 m × 150 m × 90 m underwater model. They reported an average absolute error of localization of 2.5 mm. In the same model, our proposed ELSUCATS was tested, and the average absolute error of 5.7 mm was achieved. It is believed that our result was quite comparable to Ameer and Jacob's, considering real-world problems because this small error level (a few mm) makes no difference in the real situation. Furthermore in our local search, the achievable minimum error is about 2.5 mm, as described in Section II-2.

4. Discussion

We conducted a thorough simulation study to demonstrate the feasibility of our proposed ELSUCATS. We found that our scheme outperformed the conventional ToA localization scheme (RLS) in terms of various performance measures: success rate, absolute error, mean error ratio, with noise or clean. Furthermore, our simulation was conducted in the model representing the East Sea of South Korea, which may prove the feasibility of the ELSUCATS for the UASN in a realistic environment.

Under various noise levels, sensor localization was tested.

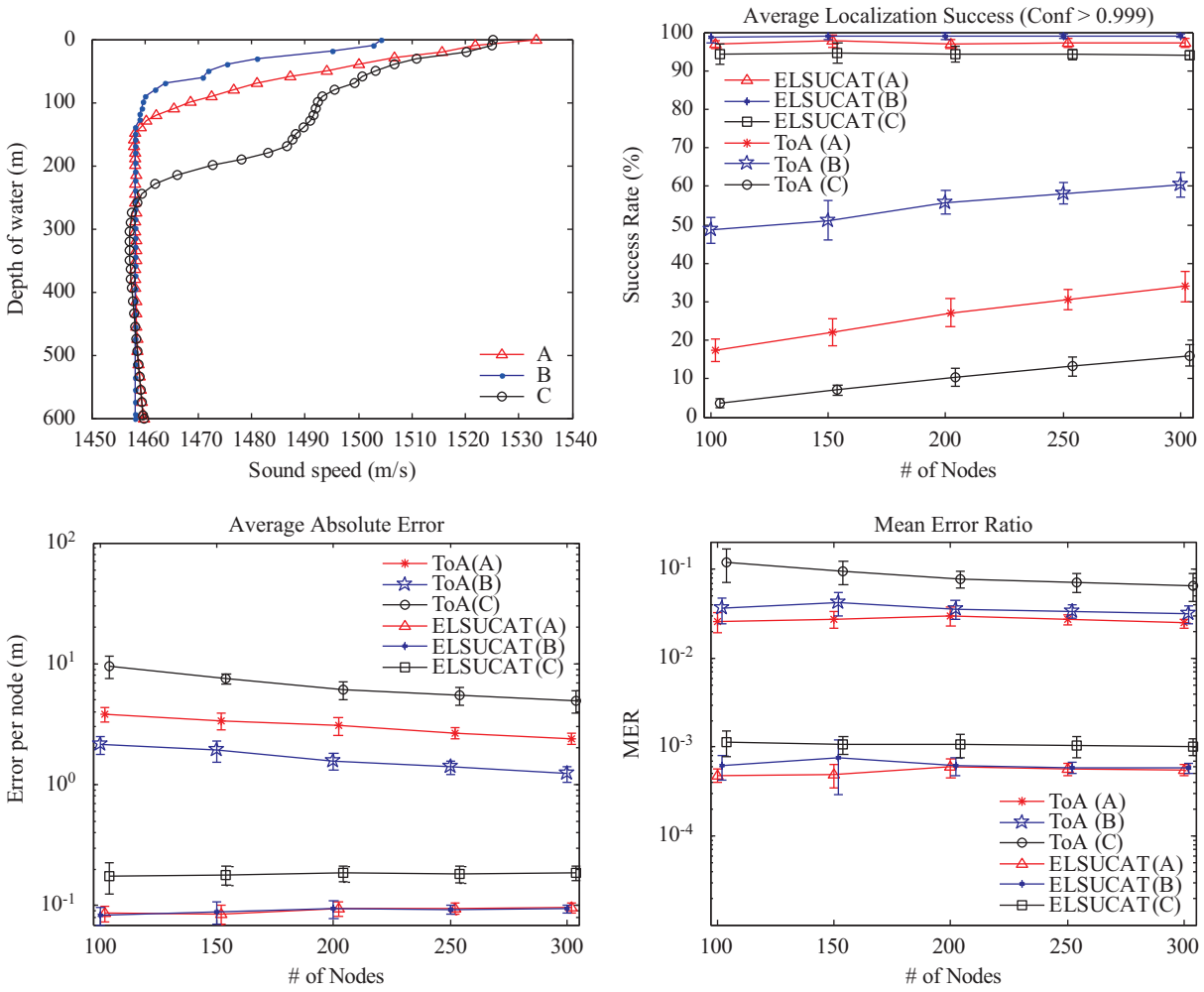

Fig. 8. Three kinds of sound speed profiles (upper left) and comparison of the simulation result of the UASN localization; average localization success rate (upper right), absolute error with three sound speed profile data (lower left), and mean error ratio of the localization result with common ToA method (lower right).

Our proposed ELSUCATS showed gradual performance improvement in noise-free cases as the number of sensor nodes increased (Fig. 6, blue lines). However, for noisy cases, no performance improvement or small degradation was observed as the number of sensor nodes increased. This observation may be due to a discrepancy of the signal-to-noise ratio (SNR) distributions among the different simulation settings (the number of sensor nodes). When the number of sensor nodes is increased, communication between anchor and sensor nodes may have a smaller arrival time measurement. However, timestamp noise (1σ or 2σ, σ was fixed) is simply added to arrival time regardless of magnitude of the arrival time. Thus, a slightly fewer SNR problems are likely to be generated as the number of sensor nodes is increased. As shown in the lower right of Fig. 7, the SNR distribution moves slightly to the left (goes lower) as the number of sensor nodes and noise level increases.

For severely noisy cases ($+5\sigma$, not shown here), the localization performance dropped to a 91.5% success rate and a 35-cm averaged absolute error. However, this drop may be not that severe, so our scheme may be considered as having strong robustness to noise.

Our UASN system response time showed a gradual decrease as the numbers of sensors and anchors both increased. Average traveling time of the localization request signal also decreased when the density of sensor nodes increased.

According to the definition of response time, which is time elapsed from event detection to the localization success, response time includes the computation time for generating a constant arrival time surface, solving a least squares problem, searching for the optimal point and traveling time of localization request signal. This result seems to be reasonable, even though it may vary with the capacity of the computing resource.

From Fig. 6 (response time), we may guess how many sensor nodes and anchor nodes are required to perform the localization process under the given response time threshold. Thus, it may be possible to design an optimal UASN monitoring system based on our simulation study. Under our simulation environmental setting (as tabulated in Table 1), we suggest the UASN

monitoring system that uses 200-250 sensor nodes and 8%-12% anchor ratios.

In comparison with existing methods, ELSUCATS far outperformed the common ToA and yielded more robustness to the sound speed profile variation. Even the common ToA method yielded mild performance variations over the number of sensor nodes, while ELSUCATS showed a steady performance.

Even though a variation of SSP by depth may affect localization performance in both ELSUCATS and the common ToA method, ELSUCATs yielded small variations of localization performance. It is quite supportive that the consideration of SSP in a broad underwater environment is of great importance.

In the 150 m × 150 m × 90 m underwater model, our proposed ELSUCATS yielded somewhat lower accuracy than Ameer and Jacob's model. However, we believe ours was comparable in that ELSUCATS achieved an average absolute error of 5.7 mm; Ameer and Jacob's yielded 2.5 mm. This tiny difference is less meaningful in the real-world context. In addition, Ameer and Jacob used a simplex search to find an optimal position of sensor localization, while our method used a local grid search algorithm with 2.5 mm spatial resolution limitation for optimization. Thus, when a finer local grid search is applied, a better result is expected.

V. CONCLUSION

For large-scale UASN localization problems, the event-driven localization scheme using constant arrival time surfaces (ELSUCATS) while considering the variations of sound speed by depth was proposed and tested with the East Sea sound speed profile data in a realistic deep and broad test bed. Our scheme showed strong robustness to the timestamp error and sound speed profile variations. Furthermore, the localization success rate was steadily high, and the mean error ratio was far better than in the conventional RLS scheme. Finally, our proposed ELSUCATS looks promising for large-scale UASN localization problems.

ACKNOWLEDGEMENTS

This research has been performed as a collaborative research project of project (Supercomputing infrastructure service and application) supported by KISTI, and it was a part of the project titled "Development of Ocean Acoustic Echo Sounders and Hydro-Physical Properties Monitoring Systems," funded by the ministry of Oceans and Fisheries, Korea.

REFERENCES

Ameer, P. M. and L. Jacob (2010). Localization Using Ray Tracing for Underwater Acoustic Sensor Networks. IEEE Communications Letters 14, 930-932.

Dargie, W. and C. Poellabauer (2010). Fundamentals of Wireless Sensor Networks, John Wiley & Sons, Ltd, Hoboken

Erol-Kantarci, M., S. Oktug, L. Vieira and M. Gerla (2011). Performance Evaluation of Distributed Localization Techniques for Mobile Underwater Acoustic Sensor Networks. Ad Hoc Networks 9, 61-72.

Isik, M. T. and O. B. Akan (2009). A three dimensional localization algorithm for underwater acoustic sensor networks. IEEE Transactions on Wireless Communications 8, 4457-4463.

King, P., R. Venkatesan and C. Li (2008). An Improved Communications Model for Underwater Sensor Networks. IEEE Global Telecommunications Conference 2008, 1-6.

Liu, B., H. Chen, Z. Zhong and H. V. Poor (2010). Asymmetrical Round Trip Based Synchronization-free Localization in Large-scale Underwater Sensor Networks. IEEE Transactions on Wireless Communications 9, 3532-3542.

Mackenzie, K. V. (1981). Nine-term equation for sound speed in the oceans. The Journal of the Acoustical Society of America 70, 807-812.

Moradi, M., J. Rezazadeh and A. S. Ismail (2012). A Reverse Localization Scheme for Underwater Acoustic Sensor Networks. Sensors 12, 4352-4380.

Porter, M. B. and H. P. Bucker (1987). Gaussian beam tracing for computing ocean acoustic fields. The Journal of the Acoustical Society of America 82, 1349-1359.

Sozer, E. M., M. Stojanovic and J. G. Proakis (2000). Underwater acoustic networks. IEEE Journal of Oceanic Engineering 25, 72-83.

Teymorian, A. Y., W. Cheng, L. Ma, X. Cheng, X. Lu and Z. Lu (2009). 3D Underwater Sensor Network Localization. IEEE Transactions on Mobile Computing 8, 1610-1621.

Zhou, Z., J.-H. Cui and S. Zhou (2007). Localization for Large-Scale Underwater Sensor Networks. In NETWORKING 2007. Ad Hoc and Sensor Networks, Wireless Networks, Next Generation Internet, I.F. Akyildiz, R. Sivakumar, E. Ekici, J. C. de Oliveira, and J. McNair, eds. Springer, Berlin Heidelberg, 108-119.